Atmos. Chem. Phys. Discuss., 6, 8069–8095, 2006
www.atmos-chem-phys-discuss.net/6/8069/2006/

Atmospheric Chemistry and Physics Discussions

Intraseasonal variations of upper tropospheric water vapor in Asian monsoon region

R. Zhan[1], J. Li[1], and A. Gettelman[2]

[1]State Key Laboratory of Numerical Modeling for Atmospheric Sciences and Geophysical Fluid Dynamics (LASG), Institute of Atmospheric Physics, Chinese Academy of Sciences, Beijing, China
[2]National Center for Atmospheric Research, Boulder, CO, USA

Received: 23 May 2006 – Accepted: 7 July 2006 – Published: 24 August 2006

Correspondence to: J. Li (ljp@lasg.iap.ac.cn)

Abstract

This study investigates intraseasonal oscillations (ISOs) of upper tropospheric water vapor (UTWV) in the Asian monsoon region in boreal summer by using data with high spatial and temporal resolution from the AIRS instrument. There are robust intraseasonal cycles with periods of 30–60 days and 10–20 days in the UTWV field over both South Asia and East Asia. The 30–60-day oscillation accounts for more than 60 percent of the total variance. For the 30–60-day mode, the source and propagating signature of the UTWV disturbances are distinct in two monsoon sub-systems. Two patterns in the 30–60 day oscillation are seen: a South Asian pattern that originates on the western side of the Arabian Sea and moves eastward, and an East Asian pattern that develops over West Pacific and moves westward. The 10–20-day mode exhibits a uniform westward propagating signature from West Pacific to the Arabian Sea. The Asian summer monsoon region is identified as a main source for UTWV, so another special interest in this study is the relationship between monsoon activity and the 30–60-day oscillation of UTWV. The data show that the upper troposphere is moistened following intense monsoon convection with lags about 5–10 days. An examination of the low level circulation reveals that wet and dry periods in UTWV are closely related to active and break (inactive) periods in monsoon convection, suggesting that the Asian summer monsoon plays an important role in the intraseasonal variations of UTWV. Similar variability is seen in water vapor from European Center for Medium-Range Weather Forecasts (ECMWF) analyses.

1 Introduction

Upper Tropospheric Water Vapor (UTWV) is a key greenhouse gas which exerts a major influence on the energy balance of the earth–atmosphere system. Water vapor is also important for atmospheric chemistry as the major source of the hydroxyl radical, the primary oxidant in the troposphere. UTWV is also a valuable tracer of atmospheric

motions (e.g., Rodgers et al., 1976; Appenzeller and Norton, 1996), and transports significant amounts of energy in the form of latent heat. Consequently, UTWV has been a focus of much interest in recent years (e.g., Stratospheric Process and Their Role in Climate (SPARC), 2000).

The Asian monsoon region is the main source of UTWV between May and September (e.g., Dethof et al., 1999; Gettelman et al., 2004a; Randel and Park, 2006). About 75% of the total net upward water vapor flux at tropopause levels is contributed by the Asian monsoon circulation from July to September (Gettelman et al., 2004a). Traditionally, two sub-systems of the Asian summer monsoon can be distinguished: the South Asian summer monsoon (SASM) and the East Asian summer monsoon (EASM) with a boundary between them at roughly 90°–100° E. These two regions have their own circulation patterns and independent climate behaviors (Tao and Chen, 1987). It is possible that the signatures of UTWV variations in East Asia differ significantly from those in South Asia.

The Asian summer monsoon is well known for its prominent subseasonal variations – the active and break monsoons (e.g., Krishnamurti and Bhalme, 1976) – and the abrupt changes during its seasonal evolution, which are directly associated with intraseasonal oscillations (ISOs). The ISOs in the Asian summer monsoon have been found to be mainly controlled by a 30–60-day oscillation (e.g., Yasunari, 1979; Krishnamurti and Subrahmanyam, 1982; Lau and Chan, 1986). In addition, 10–20-day oscillation has also been suggested to contribute to the SASM (Krishnamurti and Ardanuy, 1980) and the EASM (Chan et al., 2002; Zhou and Chan, 2005). Randel and Park (2006) have shown that transient monsoon convective events play an important role in the vertical transport of water vapor into the upper troposphere.

Traditionally, discussion of ISOs has focused on the characteristics of the boreal winter ISO in the tropics (also called the Madden-Julian Oscillation, or MJO). The monsoon active and break periods are also strictly speaking "intraseasonal oscillations", and here we characterize variability in UTWV as an "ISO" to try to better understand the variability of the Asian monsoon complex. We do not equate it with the tropical

ISO or MJO which is an equatorial wave mode response to tropical heating, but we will analyze it using a methodology often employed to examine the MJO (Clark et al., 1998; Eguchi and Shiotani, 2004). Since the summertime water vapor field in the upper troposphere often exhibits a monsoon signature as mentioned above, it seems significant to document UTWV variability associated with the ISO in the Asian monsoon region. This study will therefore address the space-time variations of UTWV in the monsoon region by using AIRS data at high spatial and temporal resolution. We note that AIRS data have recently been used to characterize the tropical ISO (MJO) by Tian et al. (2006) and Fu et al. (2006). We will also investigate the relationships between UTWV and summer monsoon convective activity on the intraseasonal time scale and how UTWV variations may be related to the wet/dry phases and the monsoon active/break spells.

The outline of this paper is as follows: The data and methodology are described in the next section. Section 3 presents the results of the AIRS UTWV analysis followed by a comparison of propagating features with those from ECMWF. Conclusions and further discussion are presented in the last section.

2 Data and methodology

2.1 AIRS water vapor

The primary data used in this study are water vapor in the upper troposphere obtained from the Atmospheric Infrared Sounder (AIRS) instrument on the NASA Aqua satellite. AIRS has been operational since September 2002 (Aumann et al., 2003), and is the most advanced humidity sounding system ever deployed (Parkinson, 2003). We use AIRS level 3 (version 4.0) retrieval products on a daily 1° by 1° global grid at 12 standard pressure levels over 1000–100 hPa during boreal summer (defined as the period from May to September) of 2003 and 2004. AIRS UTWV retrievals describe a layer averaged water vapor mixing ratio between two pressure levels with the data archived by the bottom pressure of each layer. Thus "200 hPa" UTWV represents averaged UTWV

between 200 and 150 hPa. Validation of AIRS UTWV against in-situ aircraft indicates the data is unbiased with a standard error of about 25% up to 150 hPa (Gettelman et al., 2004b). We concentrate our analysis on the 150–200 hPa level, the highest validated level for AIRS UTWV. To ensure full global coverage, the available daily data in each grid box have been processed to 5-day (pentad) means and 5-day running means.

2.2 Other data

To supplement AIRS data, we use several other data sources. As a proxy for monsoon convective activity we use Outgoing Longwave Radiation (OLR) data as suggested by Wang and Fan (1999). OLR data with a 2.5° latitude-longitude resolution are provided by National Oceanic and Atmospheric Administration (NOAA) polar orbiting Satellites for the same periods of 2003 and 2004 as the AIRS data (Liebmann and Smith, 1996). To complement our analyses of AIRS UTWV associated with the ISOs, we use water vapor mixing ratio profiles derived by relative humidity and temperature from the 6-h European Center for Medium-Range Weather Forecasts (ECMWF) operational analysis data available on a 2.5° by 2.5° global grid on 21 standard pressure levels over 1000–1 hPa. We also analyze wind fields from ECMWF analyses. All of the above data have been averaged into pentad (5 day) means.

2.3 Methodology

In the following analysis, we highlight oscillations (ISOs) by estimating the spectra of water vapor at 200 hPa. Afterwards, we remove a seasonal trend and then apply Butterworth bandpass filters with peak response around the dominant periods (Murakami, 1979) to study the detailed structure and characteristics of UTWV associated with the ISOs. We then analyze OLR data and its relationship to UTWV. We also analyze the vertical structure of UTWV in the monsoon region and its evolution over time. Finally, we compare the analysis from AIRS with low level winds and UTWV from ECMWF analyses.

3 Results

3.1 The UTWV distribution

The global distribution of water vapor from AIRS at 200 hPa for 15–30 August 2004 is shown in Fig. 1. As previous studies (e.g., Dethof et al., 1999; Gettelman et al., 2004a) based on ECMWF or HALOE data suggested, peaks in UTWV are not found in the Inter-Tropical Convergence Zone (ITCZ) but away from the equator, associated with deep convection in the Asian monsoon region. The peak UTWV in Fig. 1 (~40 ppmv) is in widely elongated belt stretching eastward from the Indian subcontinent to East Asia, including China and southern Japan. This is different than the peak at 100 hPa observed in HALOE data (Gettelman et al., 2004a) which is located just to the northwest of the Indian subcontinent in boreal summer. Figure 1 also indicates contours of tropopause pressure (white solid lines), which suggests that UTWV in the 200–150 hPa layer in both SASM and EASM regions (to south of 40° N) is still located within the troposphere.

Figure 2 presents HovmÖller plot of water vapor at 200 hPa from May to September. The UTWV peak over South Asia mainly appears in June-August, and over East Asia from mid-May to September, which correspond to the rain seasons of India and China, respectively. It is also clear that the UTWV peak regions swing between South Asia and East Asia from the daily evolutions in boreal summer, suggesting that UTWV variations in East Asia are as variable as those in South Asia on intraseasonal time scales. However, it should be noted that the seasonal or regional averaged UTWV in East Asia is more variable than that in South Asia since the EASM has complex space and time structures (Chang, 2004), which may also the main reason of difference between Fig. 1 and the results by Gettelman et al. (2004a).

3.2 Characteristics of UTWV associated with the ISO in Asian monsoon region

To define the ISOs of UTWV in Asian monsoon region, the power spectra of UTWV in two sub-systems in 2004 are shown in Fig. 3. The highest power in UTWV over two monsoon regions is around 50 days. Another feature may be noted around 13 days. The 30–60 day (10–20 day) mode in South Asia can account for about 61% (13%) of the total variance and in East Asia for about 67% (14%) of the total variance. These two modes together explain nearly 75% of the total variance of UTWV in the Asian monsoon region in 2004. In contrast, the intraseasonal oscillation in 2003 seems weaker (not shown), confirming the strong interannual variability of the ISOs in Asian monsoon region (Teng and Wang, 2003). To study the detailed structure and characteristics of the two ISOs, 10–20-day and 30–60-day Butterworth bandpass filters (Murakami, 1979) are used in the following analyses.

Figure 4 shows HovmÖller plots of 30–60-day and 10–20-day 200-hPa water vapor averaged over 15°–25° N from May to September in 2003 and 2004. We average over latitudes of 15°–25° N because both UTWV seasonal changes and the ratio of 30–60-day variance to total variance peak here (not shown). We first focus on the 30–60-day mode in boreal summer of 2004 (Fig. 4b). The 30–60-day propagating signatures are separated into two sectors by the longitudes of roughly 95°–105° E where the SASM and the EASM interact. In South Asia, there is a strong eastward-propagating signature in the UTWV field, while in East Asia the strong propagating signal is westward. The propagating patterns are also present at other levels of the upper troposphere (not shown). Over South Asia there are two main wet phases from early June to early July and from late July to mid-August, and in East Asia, three wet periods in UTWV correspond to the EASM rainy seasons in South China, the Yangtze River valley and North China (not shown), respectively. During boreal summer of 2003 (Fig. 4a) the above 30–60-day features are also clear. It is interesting that the propagating signatures are reversed in the two monsoon regions, which is different from the previous studies with a purely eastward propagating disturbance in tropical upper tropospheric humidity field

(Clark et al., 1998; Mote et al., 2000; Eguchi and Shiotani, 2004; Clark, 2005). We note that the 30–60-day wet periods are closely related to the monsoon activity. Compared to the 30–60-day mode, the 10–20-day mode (Fig. 4c and d) exhibits a relatively single propagating signature. Water vapor anomalies in West Pacific generally propagate westward into the Arabian Sea (Fig. 4c and d). Some eastward propagation is seen in the Arabian Sea. Because of the larger power and amplitude, we will focus further on the 30–60 day mode.

Figure 5 presents the lag correlation of 10°–25° N running mean water vapor (without the band-pass filter) with UTWV averaged over 65°–75° E (Fig. 5a) and 120°–130° E (Fig. 5b). Here we focus on the year 2004. UTWV disturbances in Asian summer monsoon region consist of two patterns. One is the South Asian pattern (Fig. 5a) that originates on the western side of the Arabian Sea, propagates eastward, and dissipates in the east of the Bay of Bengal. The other pattern is the East Asian pattern (Fig. 5b) that develops over West Pacific, moves westward, and dissipates over the South China Sea. These strong eastward-propagating and westward-propagating signatures in water vapor exhibit fluctuations with a period of roughly 30–60 days. The propagating features of UTWV associated with the 30–60 day mode are distinct in two monsoon regions, and often anti-correlated.

3.3 Relationship with the Asian summer monsoon

As mentioned in the Introduction, the Asian summer monsoon likely plays an important role in the seasonal variation of UTWV. To better understand the relationship, we ask two questions. First, is the longitudinal 30–60-day oscillation of UTWV related to oscillations of Asian monsoon deep convection? If that is so, then what is the relationship between monsoon convection and UTWV? This section is aimed at addressing and discussing these two questions.

In Fig. 6, we show lag correlations of daily unfiltered OLR (10°–25° N) with OLR at 65°–75° E (Fig. 6a) and 120°–130° E (Fig. 6b). Similar to UTWV disturbances, convection also exhibits a South Asian pattern and an East Asian pattern. In South Asia

(Fig. 6a) the convective disturbance originates on the western side of the Arabian Sea and moves eastward, while in East Asia (Fig. 6b) it develops over West Pacific and moves westward. This result in Fig. 6 has been documented by previous studies based on convection from OLR and TBB (Black Body Temperature) data (Zhu and Wang, 1993; Wang and Xu, 1997) and 850-hPa kinetic energy from NCEP/NCAR reanalysis data (Chen et al., 2004). The similarity of UTWV disturbances (Fig. 5) and the OLR convective proxy (Fig. 6) suggests that the propagation of UTWV is a result of monsoon convective activity.

The relationship between monsoon convection and the longitudinal 30–60-day oscillation of UTWV is clearer when examining the vertical structure of UTWV and wind fields during the typical life cycle of the 30–60-day mode with the longitudinal distribution of filtered OLR for the same period (Fig. 7). Because the vertical wind speed is very much smaller than the horizontal wind speed and to emphasize the vertical component, the vertical wind speed has been multiplied by 200 at each level. Figure 7 shows that wet anomalies are usually accompanied by strong upward flow and enhanced convection, while dry anomalies are coincident with strong descending motion and weak convection. This point is very important because AIRS water vapor data and the satellite estimates of OLR are independent (ECMWF analyses assimilate satellite radiance data used in the OLR retrievals during this time). At pentad 40 (Fig. 7a), the enhanced moisture is located over about 100° E, and dry air can be seen over most of the SASM and EASM regions. Two pentads later (Fig. 7b), the wet anomalies over about 100° E are weakened and smaller, and positive anomalies in humidity are found over the Arabian Sea (50°–80° E) and the western Pacific Ocean (150°–170° E) but below 250 hPa. At this time, the convection is enhanced in these two regions. At pentad 44 (Fig. 7c), during the transition from the moist phase to the dry phase over about 100° E, the wet anomalies over both the Arabian Sea and the western Pacific Ocean intensify and extend up to 100 hPa. But over the Arabian Sea the anomalies move eastward, while over the Western Pacific Ocean the anomalies propagate westward. In the wind and convection fields, upward motion and enhanced convection in

these two regions move similarly to the humidity field. Four pentads later (Fig. 7e), the wet anomalies from the SASM region are weakened and converge with those from the EASM region over about 100° E. At pentad 50 (Fig. 7f), the dryness is pervasive over two monsoon regions again. Thus, it is apparent that an eastward propagation of the 30–60-day oscillation in UTWV indeed exists over South Asia and a westward propagation exists over East Asia. Another distinct feature of the ISO-related moisture variability is that water vapor above 250 hPa lags deep convection while in middle troposphere water vapor is concurrent with monsoon convection.

In the previous section, it is apparent that water vapor fields in the upper troposphere have fairly coherent relationships with the convective field in the 30–60-day band. To quantify the relationship between UTWV and convection, we calculate the lag correlations between OLR and UTWV in the 30–60 day band (Fig. 8). It is clear that the correlation pattern in the two monsoon regions is essentially similar. The main feature is that there is a vertically tilted region of significant negative correlation starting in the lower troposphere on day –5, up to 500–400 hPa on day 0, and arriving at 100 hPa on about day +10. It suggests that the low-level (high-level) moistening leads (lags) the deep convection by about 1–2 pentads, which is consistent with that observed by Kemball-Cook and Weare (2001) based on winter radiosonde data and Tian et al. (2006) based on winter AIRS data. This strong relationship between moisture and convection indicates that the upper troposphere is generally moistened following intense monsoon convection.

The monsoon ISO in UTWV is directly associated with monsoon active and break (inactive) periods in convective activity. What is the relationship between UTWV anomalies and active or break (inactive) monsoon periods? We can answer this question by examining the 30–60-day filtered 850-hPa ECMWF winds and divergence. At pentad 40 (Fig. 9a) when there is a dry phase in upper troposphere over both the SASM and EASM regions, the salient features are the prominent lowlevel anticyclonic flow over India and eastern China-western North Pacific, and the uniform low-level easterlies from the Arabian Sea to West Pacific via South China Sea. The wind over South Asia

matches monsoon break periods illustrated by Krishnan et al. (2000), and winds over East Asia are consistent with observations of inactive monsoon periods by Wang and Xu (1997). Two pentads later (Fig. 9b), weak anomalous easterlies occur over South India-Bay of Bengal and eastern West Pacific (150°–170° E), and weak cyclonic winds followed by convergence and convection form over northern Bay of Bengal and central West Pacific (140°–150° E). Note that the SASM and EASM begin an active period, when low-level converge and active convection seem account for positive humidity over the SASM and EASM regions (in Fig. 7b). At pentad 44 (Fig. 9c), the SASM and EASM reach the peak of its active period. Enhanced westerlies extend from the Arabian Sea all the way to dateline. The strong cyclonic winds over India and West Pacific are accompanied by the low-level convergence, which generally corresponds to the low OLR, indicating the dominance of deep convection over two monsoon sub-systems during this period. This matchs well with the peak of wet period. Afterwards, the SASM and EASM begin to weaken. At pentad 48 (Fig. 9e), the flow associated with a monsoon break is over South Asia, while East Asia still has weak westerlies over South China Sea and weak cyclonic winds over South China. It should be noted that the circulations over South Asia somewhat lead the weak convection (low OLR) and consequently the wet anomalies over 80°–100° E as shown in Fig. 7e, but the counterparts correspond to the wet anomalies over East Asia. At pentad 50 (Fig. 9f), the anticyclonic wind develops over 10° N and east of 100° E, and then moves northward, while the cyclonic circulation over South China weakens and finally disappears. The coherence supports the idea that the ISO of UTWV is closely related to active and break (inactive) monsoons as a whole.

3.4 Comparison of the ISO propagation between AIRS and ECMWF

To better highlight our analysis on the ISO propagating signatures in UTWV based on AIRS, water vapor from ECMWF data for the same period is compared directly to observation from AIRS. Similarly, 10–20-day and 30–60-day Butterworth bandpass filters are used in ECMWF after removing their seasonal trends.

HovmÖller plots of 30–60-day and 10–20-day UTWV similar to Fig. 4 but based on ECMWF are shown in Fig. 10. There is good agreement between the two datasets. For example, both data exhibit a strong eastward-propagating signature of UTWV disturbances in South Asia and a westward moving signature in East Asia with the boundary roughly in 90°–100° E for 30–60-day oscillation, and a relatively uniform westward propagating signature from West Pacific to the Arabian Sea for 10–20-day oscillation. In addition, main wet spells closely match in two data. However, UTWV disturbances in ECMWF seem to be larger and smoother than AIRS. The latter is likely related to the higher horizontal resolution of the AIRS product used here.

Figure 11 highlights the vertical structure of ECMWF UTWV associated with 30–60-day oscillation. Comparison between Figs. 11 and 7 suggests that the correspondence of the propagation and vertical structure of UTWV over both South Asia and East Asia are quite good. However, as mentioned above, UTWV disturbances in ECMWF seem to be larger than AIRS. Furthermore, the higher resolution AIRS product better describes the evolution of UTWV as water vapor changes rapidly in space and time. Especially at pentad 48 (Fig. 7e), AIRS exhibits weak and fragmentary wet anomalies over the Bay of Bengal, but there is no evidence of this in ECMWF data (Fig. 11e).

4 Conclusions and discussions

We have presented results that show the pronounced regionally propagating features of UTWV associated with an ISO in the Asian summer monsoon region with an emphasis on relationship to the Asian monsoon. The UTWV peak in summer lies not only in South Asia but also in East Asia, which should be noted in further intraseasonal research.

Our analysis demonstrates that intraseasonal variability of UTWV in the Asian summer monsoon region has two significant periods, a 30–60-day mode, and a 10–20-day mode. The 30–60-day oscillation of UTWV exhibits distinct patterns in the two monsoon sub-systems, defined as the South Asian pattern and the East Asian pattern,

respectively. The former originates on the western side of the Arabian Sea, followed by eastward propagation, while the latter develops over the western Pacific Ocean, followed by westward propagation. The results suggest that the 30–60-day oscillation of UTWV in the East Asian monsoon region is independent of that in the South Asian monsoon region, which may be related to the fact that the SASM and the EASM have their own circulation patterns and independent climate behavior. In fact, two main wet phases from early June to mid-August in South Asia are close to the active spells of the SASM, while three wet periods in East Asia correspond to EASM rainy seasons in South China, the Yangtze River valley and North China, respectively. The propagating features in UTWV during boreal summer of 2003 are not identical to those for the same period of 2004, suggesting that the 30–60-day oscillation of UTWV in monsoon regions has significant interannual variations. It is unclear whether such interannual variation is related to the intensity of the Asian monsoon. Compared to the 30–60-day oscillation, the 10–20-day oscillation exhibits a relatively uniform signature of westward propagation.

Like UTWV, the convection also exhibits pronounced regional patterns associated with the 30–60-day oscillation in the two monsoon systems. Further analysis shows that temporal variations of UTWV disturbances are closely coupled with the 850 hPa wind and convective proxy (OLR). Upward motion is dominant over the monsoon active region, and monsoon convection associated with the 30–60-day oscillation moistens the upper troposphere. The lag correlation pattern between OLR and UTWV in the 30–60-day band shows that high UTWV is well correlated with negative OLR anomalies, confirming the role of monsoon convection in the ISO of UTWV. When the filtered low-level winds over the two monsoon regions match the characteristics of monsoon break/inactive phase, UTWV is in the dry phase. As the monsoon break/inactive phase turns into a monsoon active phase, the adjustment of the low-level flow provides the necessary support (convergence) for transition from the dry phase into the moist phase by convergence and convection. In this sense, the Asian summer monsoon may be a crucial element in determining the sources and propagating behaviors of UTWV over

the 30–60-day timescale. Further understanding of relationship between the ISO of UTWV and monsoon convection is required.

Comparisons of UTWV between AIRS and ECMWF suggest that the propagating signature and wet spells of ISOs in ECMWF agree with those in AIRS. However, the magnitudes of UTWV disturbances in ECMWF are larger than in the AIRS data, while AIRS seems to better describe the detailed structure of the wet ISO phase.

Acknowledgements. We are grateful to L. Pan, B. Randel, M. Wen and two anonymous reviewers for their critical comments and constructive suggestions. This work was supported by the NSFC Projects (40325015, 40221503). The National Center for Atmospheric Research is supported by the National Science Foundation. This research was supported at NCAR under NASA grant EOS-03-0594-0572.

References

Appenzeller, C. H. and Norton, W. A.: Fragmentation of stratospheric intrusions, J. Geophys. Res., 101, 1435–1456, 1996.

Aumann, H. H., Chahine, M. T., Gautier, C., et al.: AIRS/AMSU/HSB on the Aqua mission: Design, science objectives, data products, IEEE Trans. Geosci. Remote Sens., 41, 253–264, 2003.

Chan J. C. L., Ai, W., and Xu, J.: Mechanisms responsible for the maintenance of the 1998 South China Sea summer monsoon, J. Meteor. Soc. Japan, 80, 1103–1113, 2002.

Chang, C. P. (Ed.): East Asian Monsoon, World Scientific Press, Singapore, 2004.

Chen, L. X., Gao, H., He, J. H., Tao, S. Y., and Jin, Z. H.: Zonal propagation of kinetic energy and convection in the South China Sea and Indian monsoon regions in boreal summer, Sci. China Ser. D, 47, 1076–1084, 2004.

Clark, H. L.: Longitudinal variability of water vapor and cirrus in the tropical tropopause layer, J. Geophys. Res., 110, D07107, doi:10.1029/2004JD004943, 2005.

Clark, H. L., Harwood, R. S., Mote, P. W., and Read, W. G.: Variability of water vapor in the tropical upper troposphere as measured by the Microwave Limb Sounder on UARS, J. Geophys. Res., 103(D24), 31 695–31 707, 1998.

Dethof, A., O'Neill, A., Slingo, J. M., and Smit, H. G. J.: A mechanism for moistening the lower stratosphere involving the Asian summer monsoon, Quart. J. Roy. Meteor. Soc., 125, 1079–1106, 1999.

Eguchi, N. and Shiotani, M.: Intraseasonal variations of water vapor and cirrus clouds in the tropical upper troposphere, J. Geophys. Res., 109, D12106, doi:10.1029/2003JD004314, 2004.

Fu, X., Wang, B., and Tao, L.: Satellite data reveal the 3-D moisture structure of Tropical Intraseasonal Oscillation and its coupling with underlying ocean, Geophys. Res. Lett., 33, L03705, doi:10.1029/2005GL025074, 2006.

Gettelman, A., Kinnison, D. E., Dunkerton, T. J., and Brasseur, G. P.: Impact of monsoon cir-10 culations on the upper troposphere and lower stratosphere, J. Geophys. Res., 109, D22101, doi:10.1029/2004JD004878, 2004a.

Gettelman, A., Weinstock, E. M., Fetzer, E. J., et al.: Validation of Aqua satellite data in the upper troposphere and lower stratosphere with in situ aircraft instruments, Geophys. Res. Lett., 31, L22107, doi:10.1029/2004GL020730, 2004b.

Kemball-Cook, S. R. and Weare, B. C.: The onset of convection in the Madden-Julian Oscillation, J. Clim., 14, 780–793, 2001.

Krishnamurti, T. N. and Subrahmanyam, D.: The 30–50 day mode at 850 mb during MONEX, J. Atmos. Sci., 39, 2088–2095, 1982.

Krishnamurti, T. N. and Bhalme, H. N.: Oscillations of a monsoon system. Part I. Observational aspects, J. Atmos. Sci., 33, 1937–1954, 1976.

Krishnamurti, T. N. and Ardanuy, P.: The 10–20-day westward propagating mode and breaks in the monsoon, Tellus, 32, 15–26, 1980.

Krishnan, R., Zhang, C., and Sugi, M.: Dynamics of breaks in the Indian summer monsoon, J. Atmos. Sci., 57, 1354–1372, 2000.

Lau, K.-M. and Chan, P. H.: Aspects of 40–50-day oscillation during the northern summer as inferred from outgoing longwave radiation, Mon. Wea. Rev., 114, 1354–1367, 1986.

Liebmann, B. and Smith, C. A.: Description of a complete (interpolated) Outgoing Longwave Radiation dataset, Bull. Amer. Met. Soc., 77, 1275–1277, 1996.

Madden R. A. and Julian, P. R.: Observations of the 40–50-day tropical oscillation – A review, Mon. Wea. Rev., 122, 814–837, 1994.

Mote, P. W., Clark, H. L., Dunkerton, T. J., Harwood, R. S., and Pumphrey, H. C.: Intraseasonal variations of water vapor in the tropical upper troposphere and tropopause region, J.

Geophys. Res., 105(D13), 17 457–17 470, 2000.

Murakami, M.: Large-scale aspects of deep convective activity over the GATE area, Mon. Wea. Rev., 107, 994–1013, 1979.

Parkinson, C. L.: Aqua: an Earth-Observing Satellite mission to examine water and other climate variables, IEEE Trans. Geosci. Remote Sens., 41, 173–183, 2003.

Randel, W. J. and Park, M.: Deep convective influence on the Asian summer monsoon anticyclone and associated tracer variability observed with AIRS, J. Geophys. Res., 111, D12314, doi:10.1029/2005JD006490, 2006.

Rodgers, E. B., Salomonson, V. V., and Kyle, H. L.: Upper tropospheric dynamics as reflected in Nimbus 4 THIR 6.7-μm data, J. Geophys. Res., 81, 5749–5758, 1976.

Stratospheric Processes and their Role in Climate (SPARC): Assessment of upper tropospheric and lower stratospheric water vapor, WCRI 113, WMO/TD-N0 1043, edited by: Kley, D., Russell III, J. M., and Phillips, C., World Meteorol. Org., Geneva, Switzerland, 2000.

Tao, S. Y. and Chen, L. X.: A review of resent research on the East Asia summer monsoon over China. Monsoon Meteorology, edited by: Chang, C.-P. and Krishnamurti, T. N., pp. 50–92, Oxford Univ. Press, New York, 1987.

Teng, H. Y. and Wang, B.: Interannual variations of the boreal summer intraseasonal oscillation in the Asian–Pacific region, J. Clim., 16, 3572–3584, 2003.

Tian, B., Waliser, D. E., Fetzer, E. J., Lambrigtsen, B. H., Yung, Y., and Wang, B.: Vertical moist thermodynamic structure and spatial-temporal evolution of the MJO in AIRS observations, J. Atmos. Sci., in press, available at: http://www.ametsoc.org/journal_abstracts/get_pta.cfm?sJcode=JAS, 2006.

Wang, B. and Fan, Z.: Choice of South Asian summer monsoon indices, Bull. Amer. Meteor. Soc., 80, 629–638, 1999.

Wang, B. and Xu, X.: Northern Hemisphere summer monsoon singularities and climatological intraseasonal oscillation, J. Clim., 10, 1071–1085, 1997.

Yasunari, T.: Cloudiness fluctuations associated with the Northern Hemisphere summer monsoon, J. Meteor. Soc. Japan, 57, 227–242, 1979.

Zhou, W. and Chan, J. C. L.: Intraseasonal oscillation and the South China Sea summer monsoon onset, Int. J. Climatol., 25, 1585–1609, 2005.

Zhu, B. Z. and Wang, B.: The 30–60-day convection seesaw between the tropical Indian and western Pacific oceans, J. Atmos. Sci., 50, 184–199, 1993.

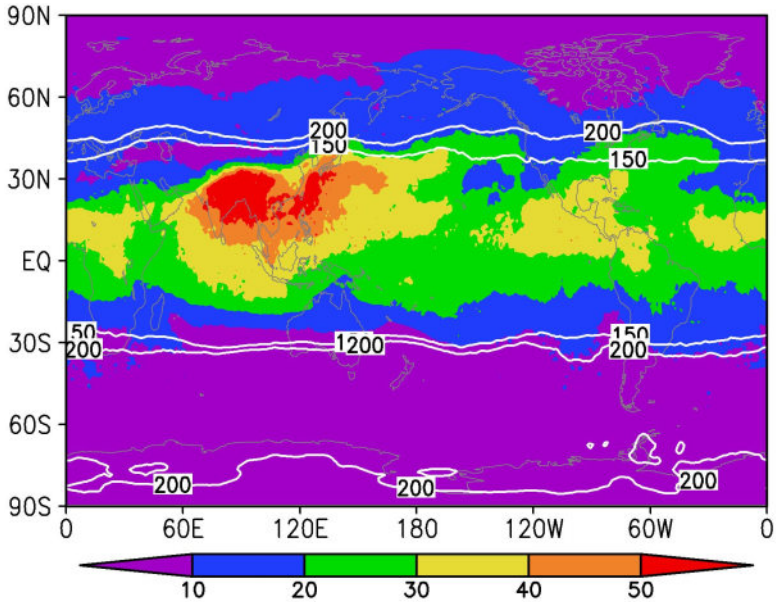

Fig. 1. Global distribution of AIRS water vapor (WV: ppmv) at 200 hPa averaged in 15–30 August 2004. White solid lines indicate contours of tropopause pressure (150, 200 hPa).

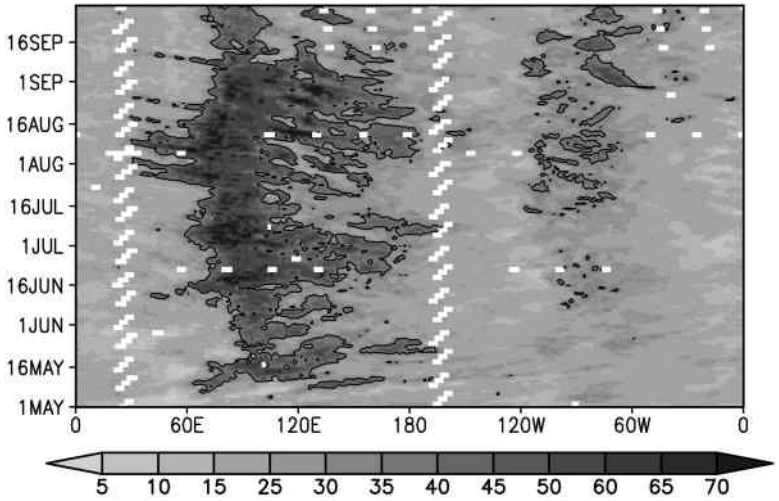

Fig. 2. HovmÖller plot of daily AIRS WV at 200 hPa averaged over 20°–30° N from May to September 2004. The black solid contours are 35 ppmv.

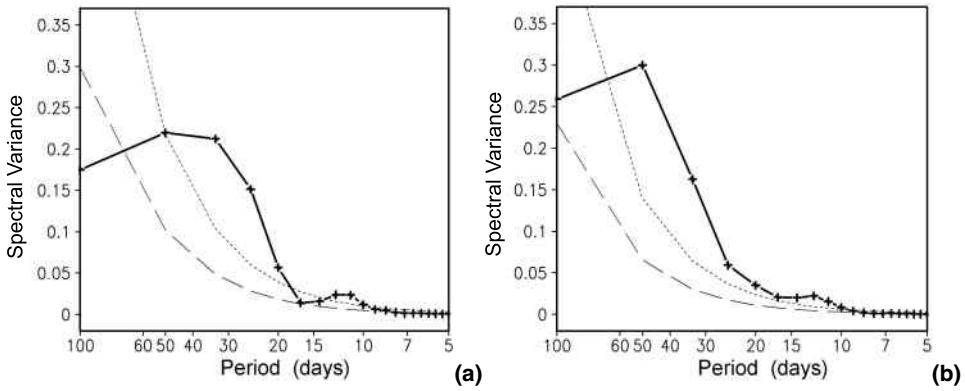

Fig. 3. Power spectra (thick solid line) for 5-day running mean 200 hPa WV in **(a)** South Asia (35°–97.5° E, 0°–22.5° N) and **(b)** East Asia (110°–140° E, 0°–40° N) from May to September 2004 based on AIRS, shown together with the spectrum density of red or white noise and the 95% confidence levels (thin dashed and dot-dashed lines, respectively).

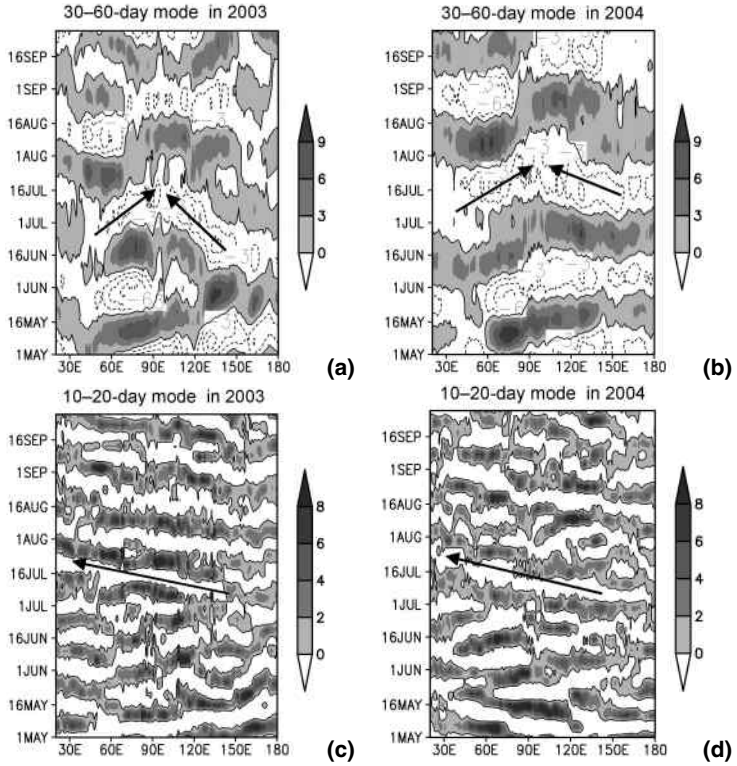

Fig. 4. HovmÖller plots of 30–60-day and 10–20-day 200 hPa WV averaged over 15°–25° N latitude from May to September in (**a** and **c**, respectively) 2003 and (**b** and **d**, respectively) 2004 based on AIRS. The solid arrow represents the propagation of enhanced (suppressed) water vapor anomaly.

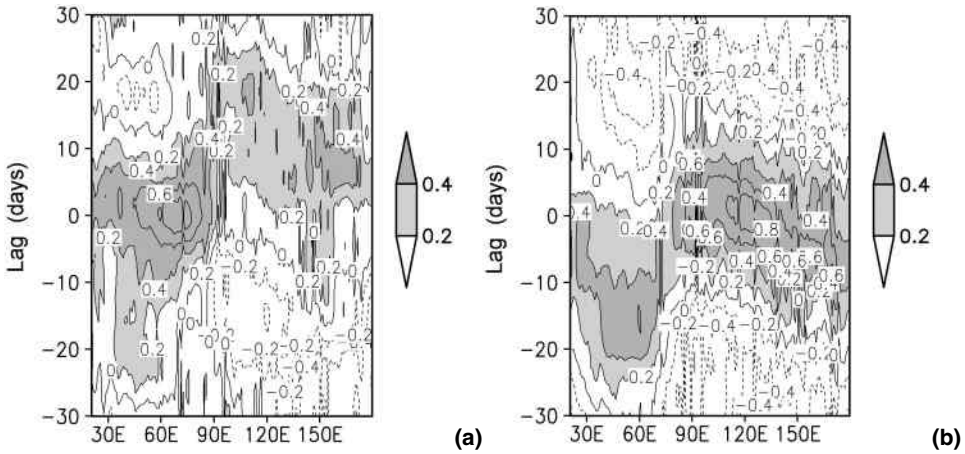

Fig. 5. Time-longitude cross-section of lag correlations of 10°–25° N 5-day running mean WV (without the band-pass filter) at 200 hPa with WV averaged over **(a)** 65°–75° E and **(b)** 120°–130° E based on AIRS. Negative lags correspond to WV averaged over 10°–25° N leading. The positive correlations significant at 99% confidence level are shaded.

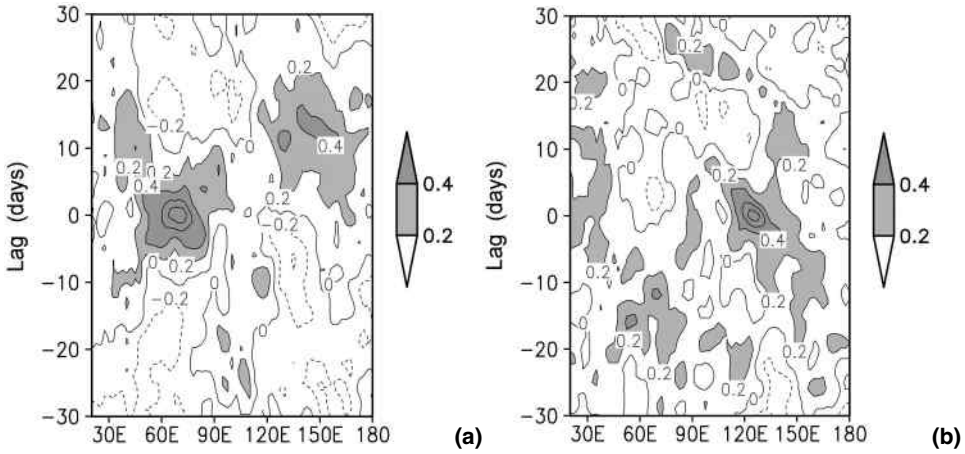

Fig. 6. The same as Fig. 5, but for daily OLR.

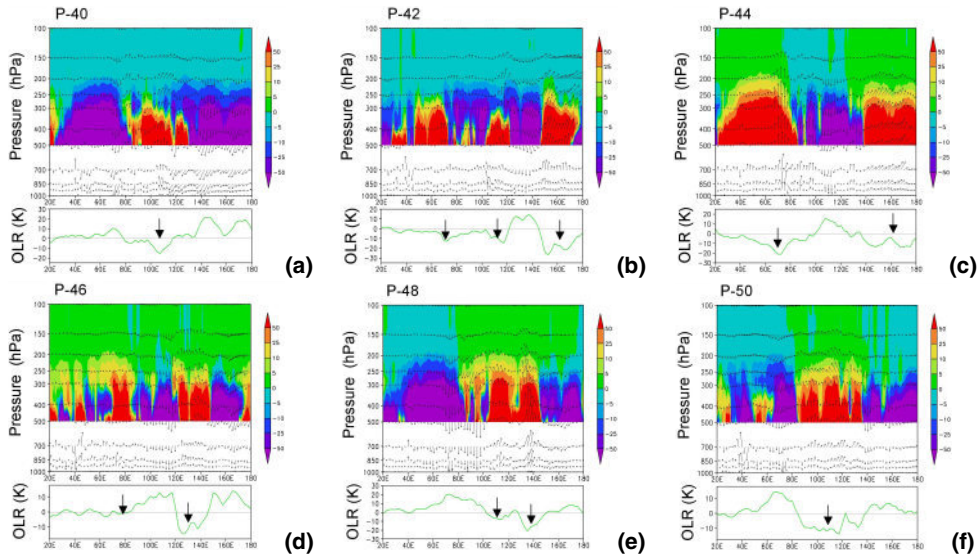

Fig. 7. (top) Longitude-pressure sections of 30–60-day filtered WV (ppmv, shading) based on AIRS and vertical wind components (vectors) at **(a)** pentad 40 (15–19 July), **(b)** pentad 42 (25–29 July), **(c)** pentad 44 (4–8 Aug.), **(d)** pentad 46 (14–18 Aug.), **(e)** pentad 48 (24–28 Aug.), and **(f)** pentad 50 (3–7 Sep.) in 2004. The reference vector is 3 m s^{-1}. (bottom) The longitudinal distribution of 30–60-day filtered OLR for the same period. The solid arrow represents the enhanced convection. All plots are for 15°–25° N.

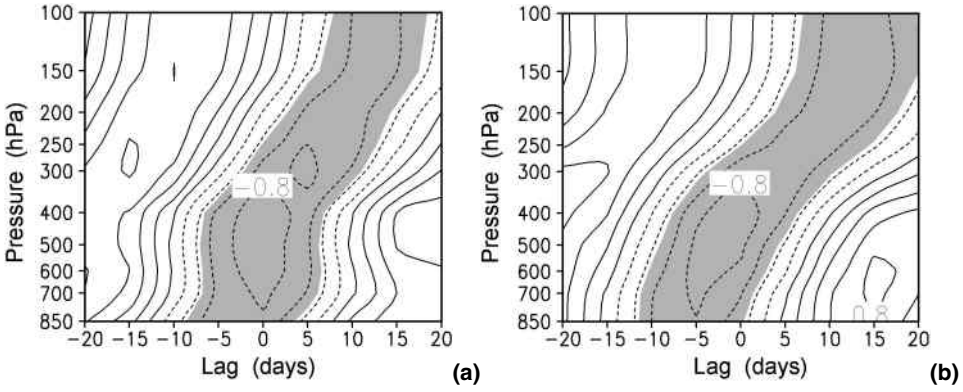

Fig. 8. Lag correlations between OLR and AIRS WV on 30–60 day band in **(a)** South Asia (35°–97.5° E, 5°–22.5° N) and **(b)** East Asia (110°–140° E, 0°–20° N) during May-September 2004. Positive lags refer to OLR leading WV. The negative correlations significant at 99% confidence level are shaded.

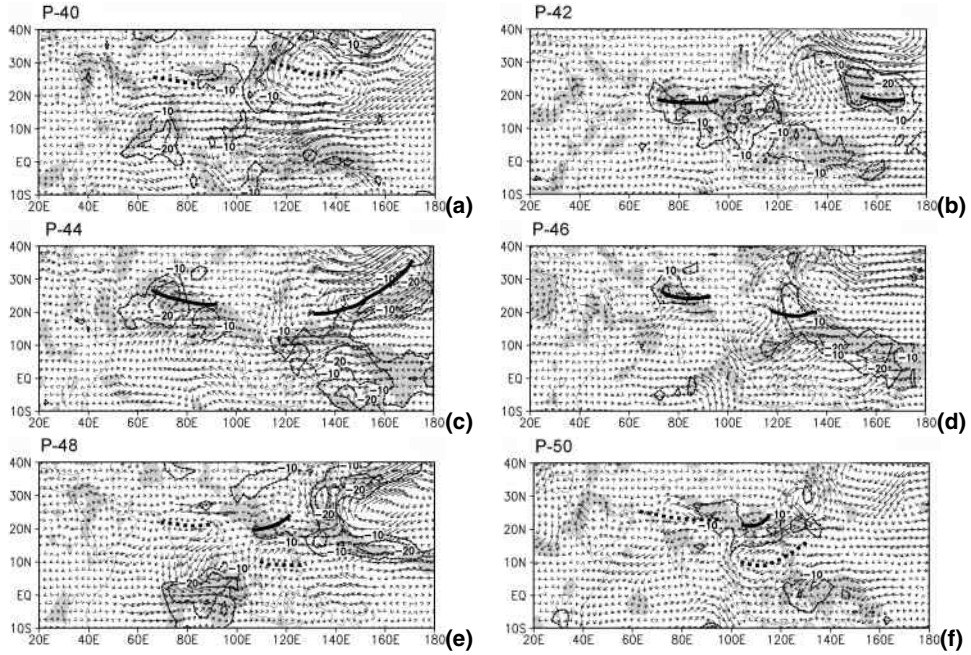

Fig. 9. The 30–60 day filtered 850-hPa winds (arrows, unit: 8 m s^{-1}) and divergence (shading) at **(a)** pentad 40 (15–19 July), **(b)** pentad 42 (25–29 July), **(c)** pentad 44 (4–8 Aug), **(d)** pentad 46 (14–18 Aug), **(e)** pentad 48 (24–28 Aug), and **(f)** pentad 50 (3–7 Sep) in 2004. The 30–60-day filtered OLR anomalies equal to –10 and –20 W m^{-2} are also shown as convective centers (thin lines). The thick solid (dashed) lines indicate trough (ridge). For divergence, only values less than or equal to -0.5×10^{-6} s^{-1} are shaded.

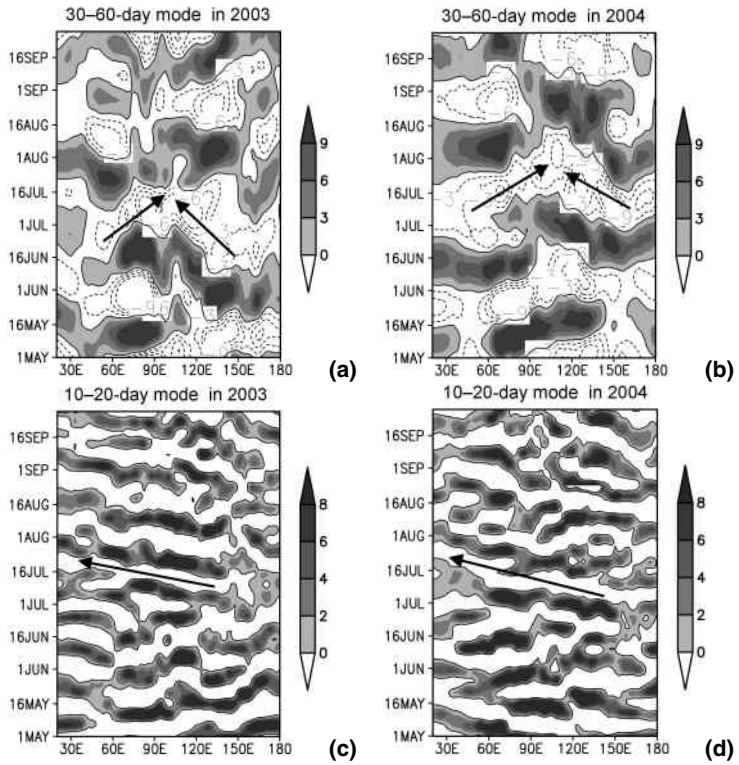

Fig. 10. As Fig. 4 but for WV based on ECMWF.

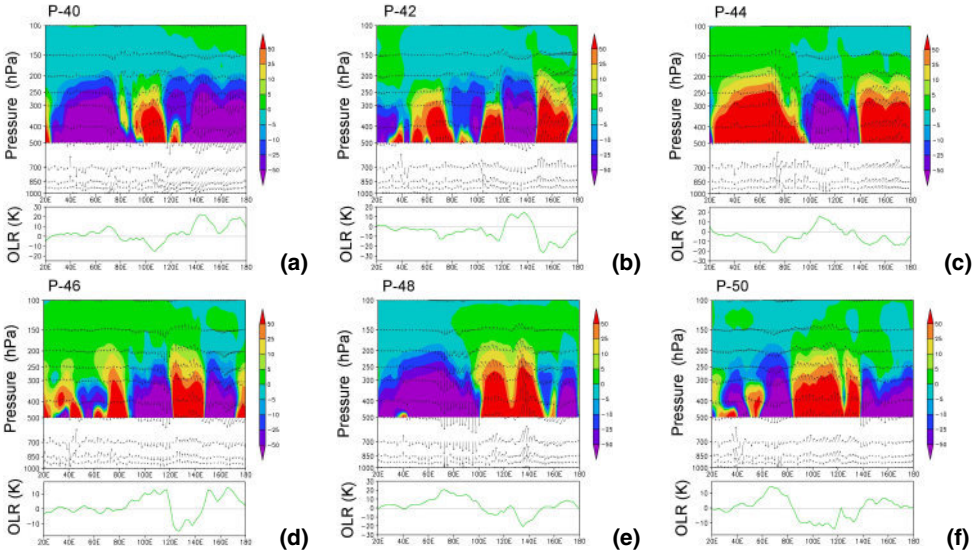

Fig. 11. As Fig. 7 but for WV based on ECMWF.